Infrared Spectroscopy of H_2S and SH in Rare-Gas Matrixes

Esa Isoniemi,* Mika Pettersson, Leonid Khriachtchev, Jan Lundell, and Markku Räsänen

Laboratory of Physical Chemistry, University of Helsinki, P.O. Box 55, FIN-00014 Helsinki, Finland

Received: September 29, 1998; In Final Form: November 25, 1998

Infrared (IR) spectra of hydrogen sulfide (H_2S), some of its complexes, and their photolysis products are studied in rare-gas matrixes (Ar, Kr and Xe) at 7.5 K. In all of these matrixes, H_2S is found to undergo hindered rotation. The vibration−rotation structures of monomeric H_2S are observed at 2651−2615, 2640−2600, and 2625−2580 cm^{-1} in Ar, Kr, and Xe matrixes, respectively. Furthermore, the H_2S dimer and the $H_2S\cdots H_2O$ complex are observed in various matrixes. Upon UV-induced decomposition of H_2S, IR absorptions of SH radical appear at 2607 cm^{-1} (Ar) and 2594 cm^{-1} (Kr). The SH radical is also observed to be complexed with H_2S (2563, 2553, and 2550 cm^{-1} in Ar, Kr, and Xe, respectively) and water (2556 cm^{-1} in Kr).

1. Introduction

Hydrogen sulfide (H_2S) is a molecule playing an important role in atmospheric chemistry as a constituent of the sulfur cycle.[1] Also, H_2S has been used as a model system for investigating different aspects of photodissociation both in the gas phase[2−16] and condensed phase.[17−19]

The IR absorption of H_2S is rather weak, which complicates its experimental study using the Fourier transform infrared (FTIR) technique. In the gas phase, the antisymmetric (ν_3) and symmetric (ν_1) stretching bands are known to center at 2628 and 2614 cm^{-1}, respectively.[20] In rare-gas matrixes, the assignments of the IR spectrum of H_2S are controversial. In an Ar matrix, the antisymmetric and symmetric stretchings were assigned at 2629.1 and 2582.5 cm^{-1} by Barnes and Howells[21] or at 2581.8 and 2568.8 cm^{-1} by Pacansky and Calder.[22] In a Kr matrix, the corresponding values are 2617.7 and 2576.0 cm^{-1} [21] compared with 2575.7 and 2566.1 cm^{-1}.[22] Tang and Brown measured the Raman spectrum of matrix isolated H_2S, and they reported the symmetric stretching at 2619 cm^{-1} in Ar matrixes.[23] In solid nitrogen, the IR spectra of monomeric H_2S, reported by different groups are in good agreement with each other.[21,23,24] The IR spectra of $(H_2S)_2$ and $H_2S\cdots H_2O$ complexes have been studied in solid Ar,[21,25] Kr,[21] and N_2.[24] In solid Ar, $(H_2S)_2$ absorbs at 2582 cm^{-1}, and in the $H_2O\cdots HSH$ complex, the S−H stretching is found at 2587 cm^{-1}.[25]

In our previous study, it was noticed that at 7.5 K monomeric H_2S possesses a number of quite narrow IR absorption lines in the S−H stretching region, for example, from 2615 to 2651 cm^{-1} for Ar matrixes,[19] which was interpreted as rotational structure.[26] In free-standing crystals of Kr and Xe, Koga et al.[27] have found that monomeric H_2S undergoes rotation as well. They assigned the rotational structure mainly to the antisymmetric stretch (ν_3). Also, the antisymmetric stretch of the hydrogen-bonded S−H in $(H_2S)_2$ was assigned at 2575 and 2573 cm^{-1} in Kr and Xe crystals. In a Kr matrix, the 2575 cm^{-1} absorption was earlier assigned to the symmetric stretch of the acceptor H_2S of $(H_2S)_2$ by Barnes and Howells.[21]

Photolysis of H_2S has been examined to a great extent both theoretically[2−9] and experimentally,[10−16] mostly in the gas phase. The first electronic absorption band of H_2S lies in the ∼180−270 nm region with an absorption maximum near 193 nm, being due to the $A^1B_1-X^1A_1$ transition.[10] The bound $^1B_1$ state and the repulsive $^1A_2$ state cross each other in the Franck−Condon region leading to predissociation of the $^1B_1$ state via the $^1A_2$ surface.[2,5] The main photodissociation channel of H_2S yields $SH(X^2\Pi_{3/2,1/2})$ radicals in the vibrational ground state[2,11,12] with cold rotational state distribution.[2,7,9] Irradiation at 193 nm excites a SH radical to the repulsive $^2\Sigma^-$ and $^2\Delta$ states, which lead to direct dissociation.[15] SH radicals are also known to predissociate in the gas phase under UV excitation at the $A^2\Sigma^+-X^2\Pi$ transition via the $^4\Sigma^-$ state.

In rare-gas solids, a number of studies on the photolysis of H_2S has appeared.[17−19,28,29] Photodissociation dynamics studies of H_2S by Zoval et al.[17,18] give two dissociation channels: (I) SH + H and (II) S + H_2. Both dissociation channels have nearly equal quantum yields when dissociation wavelength is around 225 nm, but at 193 nm dissociation channel I is dominant due to more probable exit of the H atom from the rare-gas cage. In fact, in our study of H_2S photolysis employing 193 nm radiation in low-temperature matrixes, channel II was not observed at all.[19] Also, in the gas phase, channel II has not been observed, which indicates that it is completely a cage-induced reaction which can depend on matrix morphology. The IR absorption appearing at 2540.8 cm^{-1} in the photolysis of H_2S in an Ar matrix was assigned to the SH radical,[28,29] but recently we have suggested an alternative assignment at 2607 cm^{-1}.[19]

According to Zoval et al.,[17,18] the electronic predissociation of SH(A) radical is blocked in Ar and Kr matrixes. Nevertheless, the photodissociation of SH radicals in a Kr matrix was experimentally observed while exciting at 332 nm.[18] Two-photon dissociation via ionic potentials was tentatively suggested as responsible for this process, because it was absent in an Ar matrix. Later, this photodissociation was found to happen at other SH vibration resonances as well but not between them.[19]

Although the majority of the molecules do not rotate in solid matrixes, several small molecules and radicals undergo nearly free or hindered rotation. A water molecule shows almost unhindered rotation in solid argon, and the time dependence of the absorption intensities of different transitions was interpreted to originate from the slow nuclear spin conversion of the ortho−para equilibrium from room temperature to matrix temperature

* Corresponding author. E-mail: isoniemi@csc.fi.

10.1021/jp9838893 CCC: $18.00
Published on Web 01/27/1999

equilibrium.[30−36] Also, HF,[37] NH_3, and ND_3[38] undergo almost unhindered rotation in solid argon. In solid nitrogen, NH_3 and ND_3 molecules librate.[39] CH_4 has a hindered vibration−rotation spectrum in Ar, Kr, and Xe matrixes,[40] and the time dependence of the absorption intensities is due to the nuclear spin conversion.[41,42] In solid Kr, SO_2 shows rotational motion only in the asymmetric vibration.[43] In Ar matrixes, HNCO rotates only around one inertial axis.[44] Apkarian and Weitz[45] used rotational analysis for the experimentally observed hindered rotation of CH_3F in octahedral potential field. CN radicals undergo strongly hindered rotation in rare-gas matrixes, and the rotational constants decrease by 35% and 14% from the gas-phase value in Kr and Xe matrixes, respectively.[46] In rare-gas matrixes and free-standing crystals of Kr and Xe, H_2S has been observed to rotate.[19,26,27]

Rotation in the rare-gas lattices can be treated by the crystal field model or by the rotation-translation coupling (RTC) model.[47−52] In the crystal field model, perturbation on the molecule is created by electrostatic barrier exerted by the environment;[45] i.e., the octahedral potential field of the rare-gas lattice splits and shifts the rotational levels. There exists a number of studies on rotation of molecules in octahedral field[48,49] for linear,[50] regular tetrahedron,[51] and symmetric top molecules.[45] General group theory consideration for matrix isolated molecules at a site of a crystal field of any symmetry was presented by Miller and Decius.[52] The RTC model considers additionally the coupling between molecular translation and rotation, which is due to the difference between the molecular center of mass and the center of electrical interaction.[45]

In this work, IR spectra of H_2S and some of its complexes and photolysis products are studied in solid rare-gas matrixes (Ar, Kr, and Xe) at 7.5 K. In all of these matrixes, H_2S is found to undergo hindered rotation. The vibration−rotation spectra are simulated by using an approach of reduced rotational constants. The IR absorption of SH radicals is reliably assigned in Ar and Kr matrixes, and the IR absorptions of complexes of SH are reported in Ar, Kr, and Xe matrixes. This work is partially motivated by our present attempts to experimentally investigate photolysis of H_2S_2 in rare-gas matrixes. Because H_2S is the only thermodynamically stable molecule of hydrogen sulfides (H_2S_x),[53] it is always present in H_2S_2 samples, and contradictory data on H_2S complicate the interpretation of such studies.

2. Experimental Section

Mixtures of hydrogen sulfide (H_2S) with rare gases were prepared by standard manometric procedures. H_2S of 99.85% purity (Merck), Ar of 99.9999%, and Kr and Xe of 99.997% purity (Aga) were used without purification. Gas mixtures were sprayed onto a CsI substrate through a $^1/_{16}$ in. capillary in various proportions (M/A = 300−2000). During deposition, the substrate temperature was 7.5 K for Ar, 20 K for Kr, and 30 K for Xe matrixes. After the deposition of Kr and Xe matrixes, the temperature was slowly lowered to 7.5 K. A closed-cycle helium cryostat (DE-202, APD) was used for cooling. The temperature was measured by a silicon diode (accuracy 0.5 K), and a resistive heater was used to control temperatures. In annealing, Ar and Kr matrixes were typically heated to 30 K, and Xe matrixes to 50 K.

H_2S was photolyzed by an excimer laser (ELI 76, Estonian Academy of Science) at 193 nm (ArF) with pulse energies of 5−20 mJ and pulse duration of ∼10 ns. Selective decomposition of SH radicals was achieved by doubled radiation of an optical parameter oscillator (OPO Sunlite with FX-1, Continuum) with pulse energy of ∼10 mJ in the UV and the pulse duration of 5−7 ns. Photolysis products were monitored by measuring IR absorption spectra or laser-induced fluorescence (LIF). The IR spectra were used for the detection of H_2S and SH and their complexes, and luminescence spectra were used to detect SH, S and S_2.[19]

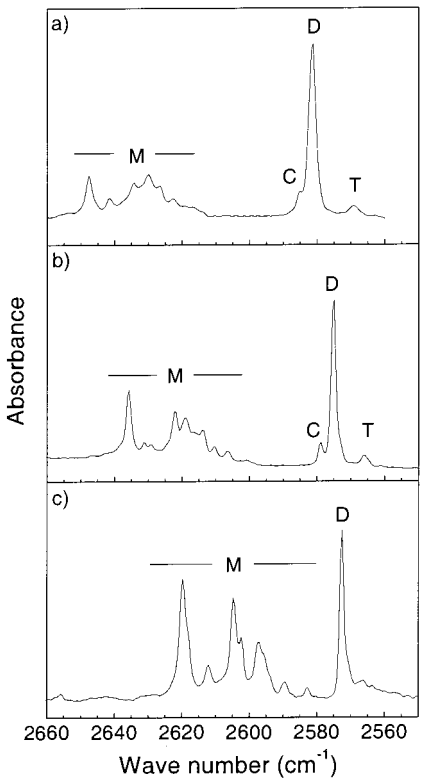

Figure 1. Stretching region of H_2S in (a) Ar, (b) Kr, and (c) Xe matrixes. M is the H_2S monomer, C is the $H_2S\cdots H_2O$ complex, D is the H_2S dimer, and T is the H_2S trimer. The resolution is 1.0 cm^{-1}, and the M/A ratio is 300.

The IR spectra were measured by using a Nicolet 60SX FTIR spectrometer with resolution of 0.25 or 1 cm^{-1} co-adding 100−500 scans for one FTIR spectrum. The luminescence spectra were measured by a single spectrometer (Spex 270M, resolution 0.3 nm) equipped with a gated ICCD camera (Princeton Instruments). OPO radiation was used for electronic excitation in LIF measurements. The wavelength of the OPO radiation was monitored by a pulsed wave meter (WA-4500, Burleigh) with accuracy of 0.1 cm^{-1}. The pulse energy was measured by a laser power meter (MAX 5200, Molectron).

3. Infrared Spectra of H_2S

3.a. Experimental Results. In Ar, Kr, and Xe matrixes, several IR absorption features of H_2S were observed in the S−H stretching region around 2600 cm^{-1}, as shown in Figure 1. IR absorption spectra of H_2S in symmetric and antisymmetric stretching regions show complex fine structures, marked with M, in the 2651−2615, 2640−2600, and 2625−2580 cm^{-1} regions in Ar, Kr, and Xe matrixes, respectively. The spacing of the absorption lines is ∼1−3 cm^{-1} in all matrixes. Additionally, relatively strong absorptions, marked with D, are seen at lower wavenumbers 2582, 2575, and 2573 cm^{-1} in Ar, Kr, and Xe matrixes, respectively. In Ar and Kr matrixes, the strong absorption D has a sideband, marked with C, at higher wavenumbers 2586 and 2579 cm^{-1}, respectively. Weaker absorptions, marked with T, are seen at lower M/A ratios in Ar and Kr matrixes at 2577 and 2566 cm^{-1}, respectively. In the H_2S bending region only very weak absorptions are observed.

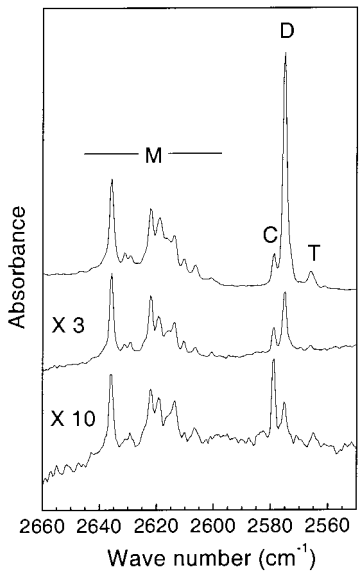

Figure 2. M/A dependence of H_2S absorptions in a Kr matrix. The upper trace M/A = 300, the middle trace M/A = 1000, and the lower trace M/A = 2000. The notation and resolution are the same as in Figure 1.

Figure 2 shows the M/A ratio dependence of the IR spectrum of H_2S in Kr matrixes. The ratios of the gas mixtures are 300, 1000, and 2000 in the upper, middle and lower trace, respectively. The intensity of absorptions M shows roughly linear dependence on the M/A ratio. The absorption intensity of D have higher order dependence on the M/A ratio, whereas the absorption intensity of C shows less systematic dependence. In concentrated matrixes (M/A = 300), the absorption T becomes visible. The M/A ratio dependence is similar in Ar, Kr, and Xe matrixes, and the shape of the M structure is M/A ratio independent.

These concentration dependencies and matrix shifts suggest that the absorptions M, showing a fine structure and being in the higher wavenumber region, belong to monomeric H_2S. In free-standing crystals of Kr and Xe, similar absorptions have been assigned to the vibrational−rotational absorptions of the antisymmetric stretch of H_2S monomer by Koga et al.[27]

The absorptions C and D are shifted to lower wavenumbers due to complexation of H_2S. The absorption C is assigned to $H_2S\cdots H_2O$ complex as suggested previously by Barnes et al. in an Ar matrix.[25] We also observed weak bands of the water symmetric (3589 cm^{-1}) and antisymmetric (3702 cm^{-1}) stretches in the $H_2S\cdots H_2O$ complex in Ar matrixes in accordance with Barnes et al.[25] The absorptions D originate from H_2S dimers.[25,27] The absorption T belongs most probably to H_2S trimers.

The IR absorptions of the $H_2S\cdots H_2O$ complex is assigned to 2579 cm^{-1} in a Kr matrix. According to our ab initio calculations, the absorptions of the H_2S dimers and the $H_2S\cdots H_2O$ complex are believed to originate from symmetric (ν_1) stretching of the electron acceptor H_2S in the complexes.[54] The absorptions of H_2S trimer are assigned to 2577 and 2566 cm^{-1}, in Ar and Kr matrixes, respectively.

Also, we measured the IR spectra of H_2S in Ar matrixes at different temperatures. For higher temperatures, broadening of the lines and minor intensity redistribution was observed, and the fine structure disappears at above 15 K. Due to broadening, it is difficult to make any quantitative comparisons between the spectra at different temperatures. It is important to note that the temperature dependence is reversible; i.e., the spectrum recovers its fine structure under decreasing the temperature.

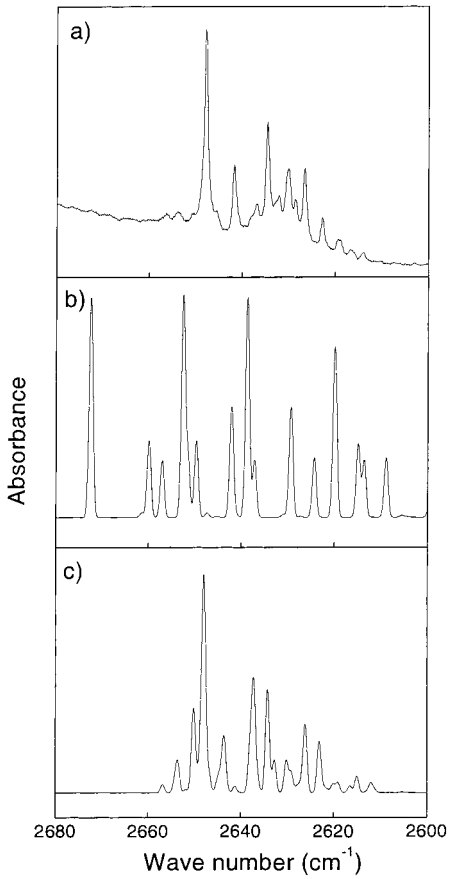

Figure 3. Simulation of a vibration−rotation spectrum of H_2S in an Ar matrix. (a) The experimental vibration−rotation spectrum of H_2S with resolution of 0.25 cm^{-1}. (b) The simulated vibration−rotation spectrum of H_2S with the gas-phase rotational constants at 7.5 K. Relative intensities of P, Q, and R branches are equal to 1. (c) The simulated vibration−rotation spectrum of H_2S, with reduced rotational constants. The line width in the spectrum is 1.0 cm^{-1}.

3.b. Simulations of the Vibration−Rotation Spectra. The fine structure M, seen in Figures 1 and 2, is clearly too complex to originate from site effects of nonrotating molecules. A natural explanation for the spectrum is the rotation fine structure like in the case of H_2O.[30−36] However, the vibration−rotation structures cannot be explained fully using the gas-phase rotational constants and allowed transitions at 7.5 K as shown in Figure 3a,b and as discussed by Koga et al.[27] In particular, experimental spacing appears to be very small when compared with the simulated structure.

We attempted to model the observed spectrum by modifying the rotational constants of the asymmetric top to fit the experimental spectra. The rotational constants were calculated by the method of combination differences with suitable assignment of the vibration−rotation transitions. Table 1 shows the assigned transitions, and those marked with ^{b} were used in the method of combination differences in Ar and Kr. This set of bands gives the rotational constants of the upper vibrational state. The rotational constants of the upper and ground vibrational states were assumed to be equal for both vibrations, because the data are too limited for obtaining the three rotational constants for both vibrational states. This assumption was made on the basis of the fact that the gas-phase rotational constants are within ± 0.2 cm^{-1} in the vibrational ground and first excited state,[20,55] which is below our resolution (0.25 cm^{-1}) and the experimental line width. However, it should be noted here that the interaction between a rotating molecule and matrix depends

TABLE 1: Experimental and Simulated Transition Wavenumbers of H_2S in Ar and Kr Matrices

		Ar		Kr	
mode	transition[a]	measd/cm^{-1}	calcd/cm^{-1}	measd/cm^{-1}	calcd/cm^{-1}
ν_3	202 221		2643.4	2632.0	2632.0
ν_3	111 110	2647.8	2647.9	2635.8	2635.8
ν_3	110 111	2647.8(s)	2649.1	2635.8(s)	2637.8
ν_3	211 212	2650.6	2650.2	2635.8(s)	2639.9
ν_3	322 303	2653.9(s)	2654.2		2641.6
ν_3	221 202	2653.9	2653.6		2643.0
ν_3	331 312	2656.4	2656.8		2643.4
ν_1	321 212	2641.7	2643.8	2631.1	2631.8
ν_1	330 221	2645.5(s)	2644.7	2629.2	2630.6
ν_1	322 211	2641.7(s)	2641.3	2626.9	2626.3
ν_1	220 111[b]	2638.1	2638.0	2624.4	2623.3
ν_1	221 110[b]	2636.9	2637.2	2622.1	2621.6
ν_1	212 101[b]	2634.5	2634.2	2619.0	2618.5
ν_1	202 111	2632.2	2632.7	2616.7	2617.8
ν_1	111 000	2630.0	2630.2	2613.8	2613.8
ν_1	221 212	2628.5	2629.1	2613.8(s)	2612.2
ν_1	110 101[b]	2626.6	2626.1	2610.4	2609.1
ν_1	101 110[b]	2622.8	2623.1	2606.5	2606.6
ν_1	212 221	2622.8(s)	2620.1	2602.4	2602.9
ν_1	000 111[b]	2619.2	2619.1	2600.8	2601.3
ν_1	111 202	2616.5	2616.5		2597.2
ν_1	101 212	2614.0	2615.0		2596.6
ν_1	110 221	~2612	2612.0		2593.5

[a] The notation of the transition is $J'K'_aK'_c$ $J''K''_aK''_c$. [b] The named transitions are used in the method of combination differences. s indicates a shoulder of the absorption.

on the effective size of the rotating molecule which can lead to different constants for the ground and excited states. To estimate the transition wavenumbers, rotational energy levels were calculated with the obtained rotational constants by using the known analytic expressions for low-lying energy levels.[56]

Table 1 includes the measured and calculated transition wavenumbers in Ar and Kr matrixes at 7.5 K. Figure 3a shows the measured and Figure 3c shows the calculated vibration−rotation spectrum of H_2S assuming one matrix site in an Ar matrix at 7.5 K. The calculated vibration−rotation spectrum is obtained by assuming that the transition intensities depend on the Boltzmann distributions of the vibration−rotation ground states, the M_J degeneracy of the upper and lower levels, the type of a transition band, and the statistical weights due to nuclear spins. The Boltzmann distributions of the rotational states of the ground vibrational states are calculated at the matrix temperature (7.5 K). The symmetric stretching band of H_2S is of type B having strong R and P branches (weight 0.3) and a weak Q branch (weight 0.25). The antisymmetric stretching band is of type A having a strong Q branch (weight 1) and weak R and P branches (weight 0). Experimentally, absorption intensities do not change over time scale of 24 h, so fast conversion of the nuclear spins to matrix temperature equilibrium of the nuclear spins is assumed; i.e., population of ortho states is weighted by a factor of 3 and para states by a factor of 1. In the simulation, the intensity ratio between the symmetric and antisymmetric stretches was chosen equal to our experimental ratio between these bands.

In an Ar matrix, the reduced rotational constants *A*, *B*, and *C* appeared to be 3.5, 2.6, and 2.0 cm^{-1}, respectively, and the band origins are at 2624.6 and 2648.5 cm^{-1} for symmetric (ν_1) and antisymmetric (ν_3) stretches, respectively. A similar simulation of the vibration−rotation spectrum performed in a Kr matrix gives the reduced rotational constants of 3.9, 3.4, and 2.4 cm^{-1} for *A*, *B*, and *C*, respectively, and the band origins of 2607.5 and 2636.8 cm^{-1} for symmetric (ν_1) and antisymmetric (ν_3) stretches, respectively. In Xe matrixes, the rotational constants are difficult to be calculated with the method of combination differences because of the lack of resolved transitions, but the band origins are estimated to be at 2596 and 2620 cm^{-1} for the symmetric (ν_1) and antisymmetric (ν_3) stretching modes, respectively. By using the reduced rotational constants, the vibration−rotation structures are modestly well fitted within the resolution used.

In the gas phase, the rotational constants of H_2S are known to be $A = 10.2$ cm^{-1}, $B = 8.9$ cm^{-1}, and $C = 4.7$ cm^{-1},[20,55] differing considerably from the matrix values obtained. This difference might indicate a strong interaction between H_2S and the rare-gas lattice, which is in agreement with assumed fast relaxation of nuclear spins. Qualitatively, this considerable decrease of the rotational constants can be discussed in terms of partially connected movement of surrounding atoms. Considering the whole system of H_2S surrounded by rare-gas atoms, the effective moment of inertia of the H_2S molecule is increased from the gas phase due to the interactions with the matrix cage. It should be emphasized that the rare-gas shell is not considered to rotate with the H_2S molecule. It is interesting to compare the rotational constants obtained in Ar and Kr matrixes. We obtained larger rotational constants in Kr compared to Ar, which might show that the cage size, being larger in Kr, plays a more important role than direct interactions with the lattice atoms. Actually, the same trend was observed by Schallmoser et al. for CN radicals in Xe and Kr matrixes.[46]

The model discussed above reproduces rotational structure of the spectra quite well, but the intensity distribution is represented less satisfactory as seen in Figure 3c. Also, the real physical significance of the reduced rotational constants obtained is questionable. The antisymmetric stretch has only a Q branch, and the reason for the very small intensity of P and R branches is not clear. On the other hand, strong interaction with the lattice can have a profound effect on the intensities of the individual transitions. The model of reduced rotational constants could be refined by including, for example, matrix site effect on H_2S and nonrotating absorptions of H_2S.

To consider the problem more quantitatively, one can examine the rotation of an asymmetric top in octahedral potential field of the rare-gas lattice.[45,48−52] In this approach, low potential barriers established by interaction with the rare-gas environment cause shifts and splittings of the rotational levels. Such an analysis is quite complicated in the case of an asymmetric top and requires extensive theoretical studies.

It should be mentioned that our assignment for monomeric H_2S absorptions in Ar and Kr matrixes disagrees with those given by Barnes et al.[21,25] (see Table 2) and Koga et al.[27] but agrees reasonably well with that given by Tang and Brown.[23] The disagreement between this study and that by Barnes et al.[21,25] is probably due to a stronger complexation and higher measurement temperature in the latter. Also, the matrix shifts for the symmetric and antisymmetric stretching modes against the gas-phase values reported by Barnes et al.[25] differ by ~30 cm^{-1} compared with the matrix shifts for H_2O being quite small for both modes. Our small matrix-induced perturbations for H_2S are in reasonable agreement with the case of H_2O. Koga et al.[27] consider the vibration−rotation structure mainly due to the S−H antisymmetric stretch. This is in contradiction with the gas phase where the total band intensities for the symmetric and the antisymmetric stretches are 0.1776×10^{-19} and 0.4520×10^{-20} cm^{-1}/molecule cm^{-2}.[20] In our opinion, the assignment of the observed structure to the both vibrations is more plausible.

TABLE 2: Absorptions of H_2S and Comparison with the Literature

mode	gas phase	Ar[j]	Kr[j]	Xe[j]	Barnes et al., Ar	Barnes et al.,[c] Kr	Barnes et al.,[c] N_2	Nelander,[e] N_2
H_2S ν_1	2614.41[a]	2624.6[h]	2607.5[h]	2596[i]	2582.5[c]	2576.0	2619.5	2619.3
H_2S ν_2	1182.7[b]	1180	1176.9		1179.0[c]	1176.9		1179.6
H_2S ν_3	2628.46[a]	2648.5[h]	2636.8[h]	2620[i]	2629.1[c]	2617.7	2632.6	2630.4
H_2S dimer		2581.5	2575.2	2572.5	2582[d]	2576	2580.3[f]	2579.0[f]
							2617.8[g]	2617.7[g]
$H_2S\cdots H_2O$								
H_2S ν_1		2585.5	2579.0		2587[d]			2574.2
H_2O ν_1		3589			3590[d]			2628.1
H_2O ν_3		3702			3703[d]			
H_2S trimer		2577	2566					

[a] Reference 20. [b] Reference 60. [c] Reference 21. [d] Reference 25. [e] Reference 24. [f] Donor. [g] Acceptor. [h] Band origin of vibration−rotation band (transition 000 000). [i] Approximated band origin of vibration−rotation band. [j] Present study.

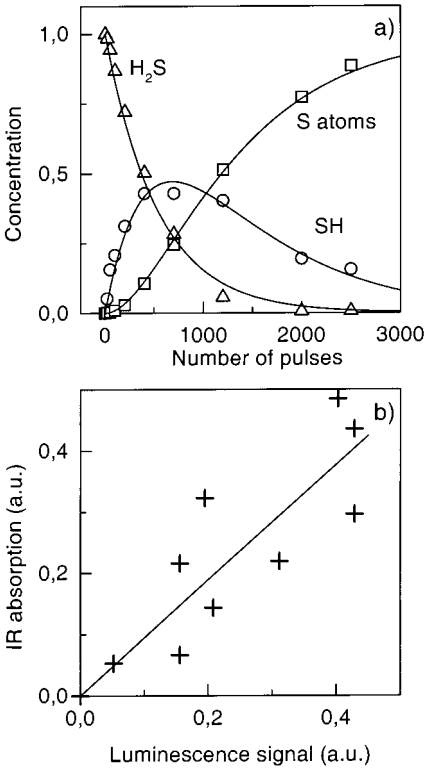

Figure 4. (a) 193 nm photolysis kinetics of H_2S in Kr matrixes. SH and S are detected by LIF and H_2S by FTIR. (b) Correlation between SH luminescence and the 2594 cm^{-1} absorption band.

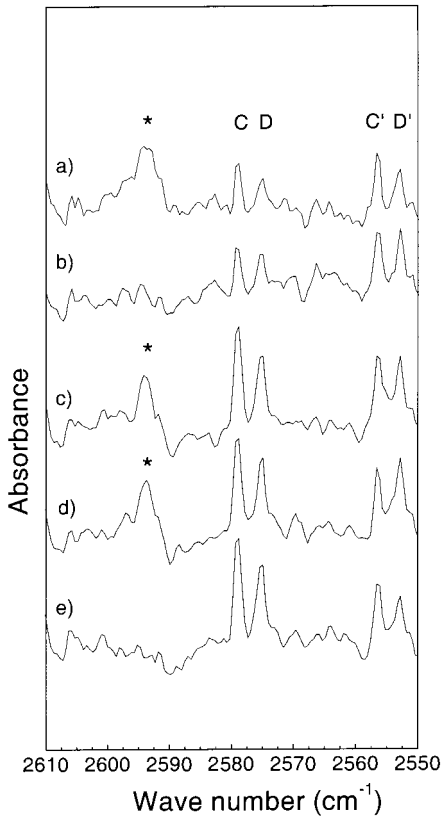

Figure 5. Identification of SH radical absorption in a Kr matrix (M/A = 1000). The SH absorption is marked by an asterisk (∗), C is the $H_2S\cdots H_2O$ complex, D is the H_2S dimer, and C′ and D′ are the complexes of SH radical. Spectrum a) is the UV-irradiated H_2S sample, and (b) and the situation after OPO radiation at 300.5 and 315.0 nm. The spectra after subsequent annealing (c), off-resonance irradiation (d), and resonance irradiation (e) are shown.

4. Infrared Spectra of the Photolysis Products

Irradiation at 193 nm in rare-gas matrixes dissociates H_2S to H atom and SH radical or to H_2 molecule and S atom. SH radicals photodissociate further to S and H atoms.[17−19] The observed kinetics of 193 nm photolysis of H_2S in a Kr matrix is shown in Figure 4a, where the H_2S concentration was measured as integrated IR absorption intensity of the monomeric lines and SH radicals and S atoms were measured by LIF. Photolysis scheme is essentially the same as in ref 19. Similar photolysis kinetics can be seen in an Ar matrix. In a Xe matrix, the self-limitation of the photolysis due to the strong absorption of 193 nm by H atoms makes the analysis more difficult.[57] Under 193 nm photolysis absorptions at 2607.0 and 2563 cm^{-1} in Ar, at 2594, 2556.4, and 2552.8 cm^{-1} in Kr, and at 2563.2 cm^{-1} in Xe matrixes appear. These absorptions are assigned to SH radical and its complexes.

To identify SH absorption in Kr matrixes, we used specific resonant decomposition of SH radicals. To remind, SH does not predissociate under UV excitation at the $A^1\Sigma^+-X^2\Pi$ transition via $^4\Sigma^-$ state in a Kr matrix, but it dissociates by a two-photon process via electronic transition (0,0) at 332.5 nm, (1,0) at 315 nm, (2,0) at 300.3 nm, etc.[17,19] Off-resonance radiation of SH, for example at 323.0 nm, has no dissociative effect on SH. Figure 5 presents the result of the experiment verifying the absorptions of SH radical. Figure 5a shows the formation of SH radical at 2590 cm^{-1}, marked with an asterisk, under 193 nm photolysis (1500 pulses) of H_2S. Resonance irradiation of SH at 300.5 nm (5000 pulses) and 315.0 nm (3000 pulses) destroys this SH absorption completely (Figure 5b). It is to be noted that also SH luminescence disappears completely during the resonance irradiation. Annealing of the matrix at 30 K regenerates the SH radical absorption at 2590 cm^{-1} (Figure 5c). Also the SH luminescence is recovered at this stage. Figure 5d shows the result of off-resonance irradiation at 323.0 nm (5000 pulses) which has effect neither on the SH absorption nor on the observed luminescence. Further resonance irradiation

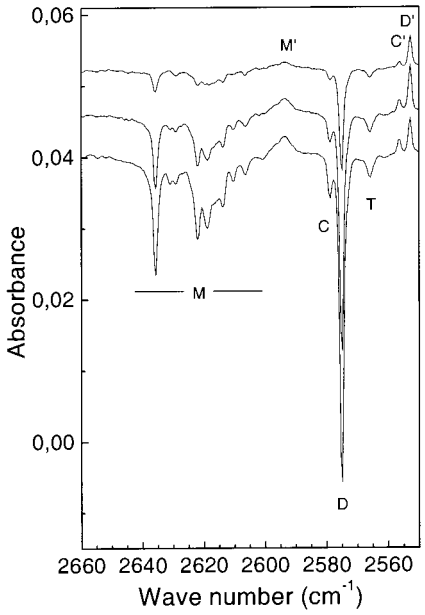

Figure 6. IR difference spectra demonstrating 193 nm photolysis of H_2S in a Kr matrix. M is the H_2S monomer, C is the $H_2S\cdots H_2O$ complex, D is the H_2S dimer, T is the H_2S trimer, M′ is the SH radical, C′ is the $SH\cdots H_2O$ complex, and D′ is the $SH\cdots H_2S$ complex.

at 332.5 nm (5000 pulses), shown in Figure 5e, destroys SH absorption and luminescence completely. It is important to note that the resonance irradiation has no effect on the other absorptions except on the absorption at 2594 cm^{-1} due to SH in solid Kr. Figure 4b demonstrates the correlation between the SH luminescence and 2594 cm^{-1} absorption band at different stages of the photolysis, which also confirms our assignment. On the basis of a natural matrix shift and photolysis kinetic correlation, the 2607.0 cm^{-1} absorption in solid Ar is assigned to the SH radical. In a Xe matrix, SH absorption was not observed, which can be explained by reduced decomposition of H_2S because of self-limitation of H_2S photolysis.[57]

In the photolysis studies by Acquista and Schoen[28] and by Barnes et al.,[29] the absorption at 2540.8 cm^{-1} was assigned to the SH radical in Ar matrix. We did not observe this absorption at all. The experiments of Acquista and Schoen[28] and Barnes et al.[29] were performed in more complexed matrixes, and the absorption 2540.8 cm^{-1} belongs possibly to some photolysis product of H_2S multimers. Furthermore, this absorption seems to be too far from the gas-phase value of the SH radical absorption at 2591.8 cm^{-1}.[58]

At 193 nm photolysis, new absorptions, in addition to those of monomeric SH radicals, were observed at 2563.2 cm^{-1} in Ar, at 2552.8 and 2556.4 cm^{-1} in Kr, and at 2550.3 cm^{-1} in Xe matrixes. Figure 6 shows the result of 193 nm photolysis of H_2S at 7.5 K in a Kr matrix. The spectra are difference spectra where an initial spectrum is subtracted from that after photolysis. The numbers of laser pulses are 1500, 3000, and 5000 in the upper, middle, and lower traces, respectively. Positive absorptions indicate the increase of products and negative absorptions show the decrease of the precursors. Assuming that the relative intensities and matrix shifts of $SH\cdots H_2S$ and $SH\cdots H_2O$ complexes are similar to those of H_2S dimers and $H_2S\cdots H_2O$ complexes, the absorption C′ at 2556.4 cm^{-1} and D′ at 2552.8 cm^{-1} in a Kr matrix (see Figure 6), can be tentatively assigned to $SH\cdots H_2O$ and $SH\cdots H_2S$, respectively. Similarly, the absorptions at 2563.2 and 2550.3 cm^{-1} are tentatively assigned to the $HS\cdots H_2S$ complex, in Ar and Xe matrixes, respectively. All SH complex wavenumbers are collected in Table 3.

TABLE 3: Absorption Wavenumbers of SH Radical and Its Complexes

	Ar/cm^{-1}	Kr/cm^{-1}	Xe/cm^{-1}
HS	2607	2594	
$HS\cdots H_2S$	2563	2553	2550
$HS\cdots H_2O$		2556	

5. Annealing

During annealing of a photolyzed Ar matrix at 30 K, recovery of SH radicals and H_2S and their complexes with H_2O and H_2S is observed. The H atoms become mobile at these temperatures in solid rare-gases, and the recovery reactions $S + H \rightarrow SH$ and $H + SH \rightarrow H_2S$ take place. Correlation between the decrease of S atoms and the increase of SH was observed during annealing.[19] After annealing of the Kr matrix at 30 K, we could not observe recovery of the monomeric H_2S molecules, but the recovery of different complexes ($SH\cdots H_2S$, $SH\cdots H_2O$, etc.) was observed. This can be due to diffusion of SH radicals or H_2S monomers and subsequent complex formation at the elevated temperatures.

It should be emphasized that in Xe matrix the result of annealing is qualitatively different from solid Ar and Kr. In addition to a very minor recovery of H_2S and $SH\cdots H_2S$, a strong absorption at 1119 cm^{-1}, with a weak shoulder at 1111 cm^{-1} and a sideband centering at 1136 cm^{-1}, was observed after annealing at 50 K. This was identified to the H−Xe stretching mode of the HXeSH molecule.[59] The formation of HXeSH explains also the small recovery of H_2S in Xe matrix during annealing.

6. Conclusions

Complex fine structures in the 2651−2615, 2640−2600, and 2625−2580 cm^{-1} regions in Ar, Kr, and Xe matrixes, respectively, are assigned to monomeric H_2S. These structures originate from vibration−rotation transitions, and they are simulated with the method of reduced rotational constants. In an Ar matrix, the band origins are at 2624.6 and 2648.5 cm^{-1} for the symmetric (ν_1) and antisymmetric (ν_3) stretches, respectively. In a Kr matrix, the values are 2607.5 cm^{-1}(ν_1) and 2636.8 cm^{-1}(ν_3). In a Xe matrix, the corresponding band origins locate approximately at 2596 and 2620 cm^{-1}.

The main dissociation channel of H_2S in rare-gas matrixes at 193 nm photolysis is $H_2S + h\nu \rightarrow SH + H$. The IR absorption of SH radical is reliably identified with simultaneous LIF and FTIR measurements. Correlation between the luminescence and IR absorption of SH radical was found, and on this basis, the IR absorption of SH radicals is assigned at 2607 and 2594 cm^{-1} in Ar and Kr matrixes, respectively. Additionally, IR absorptions of $SH\cdots H_2S$ and $SH\cdots H_2O$ complexes are tentatively assigned by assuming similar matrix behavior as for the corresponding H_2S complexes. The ν_{S-H} of the SH radical in the $SH\cdots H_2S$ complex is observed at 2563, 2553, and 2550 cm^{-1} in Ar, Kr, and Xe matrixes, respectively, and in the $SH\cdots H_2O$ complex at 2556 cm^{-1} in Ar.

During annealing of the Xe matrixes, a strong IR absorption was observed. This characteristic IR absorption at 1119 cm^{-1} is due to HXeSH, which is the first molecule containing a Xe−S bond.[59]

Acknowledgment. This work is part of a graduate school LASKEMO, and the Academy of Finland is gratefully acknowledged.

References and Notes

(1) Wayne, R. P. *Chemistry of Atmospheres*, 2nd ed.; Clarendon Press: Oxford, U.K., 1991; Chapters 1 and 5.

(2) Schinke, R. *Photodissociation Dynamics*, 1st ed.; Cambridge University Press: Cambridge, U.K., 1993; Chapter 15.
(3) Kulander, K. C. *Chem. Phys. Lett.* **1984**, *103*, 373.
(4) Theodorakopoulos, G.; Petsalakis, I. D. *Chem. Phys. Lett.* **1991**, *178*, 475.
(5) Heumann, B.; Düren, R.; Schinke, R. *Chem. Phys. Lett.* **1991**, *180*, 583.
(6) Petsalakis, I. D.; Theodorakopoulos, G. *Chem. Phys. Lett.* **1992**, *200*, 387.
(7) Heumann, B.; Weide, K.; Düren, R.; Schinke, R. *J. Chem. Phys.* **1993**, *98*, 5508.
(8) Theodorakopoulos, G.; Petsalakis, I. D.; Nicolaides, C. A. *Chem. Phys. Lett.* **1993**, *207*, 321.
(9) Gu, X.; Muñoz, L. A.; Ishikawa, Y.; Weiner, B. R. *Chem. Phys. Lett.* **1993**, *211*, 65.
(10) Watanabe, K.; Jursa, A. S. *J. Chem. Phys.* **1964**, *41*, 1650.
(11) Hawkins, W. G.; Houston, P. L. *J. Chem. Phys.* **1980**, *73*, 297.
(12) Heaven, M.; Miller, T. A.; Bondybey, V. E. *Chem. Phys. Lett.* **1981**, *84*, 1.
(13) Jackson, W. M.; Okabe, H. In *Advances in Photochemistry*; Volman, D. H., Hammond, G. S., Gollnick, K., Eds.; John Wiley & Sons: New York, 1986; Vol. 13.
(14) Weiner, B. R.; Levene, H. B.; Valentini, J. J.; Baronavski, A. P. *J. Chem. Phys.* **1989**, *90*, 1403.
(15) Hsu, C.-W.; Liao, C.-L.; Ma, Z.-X.; Tjossem, P. J. H.; Ng, C. Y. *Chem. Phys. Lett.* **1992**, *199*, 78.
(16) Kim, D.-C.; Hahn, J. W.; Lee, E. S.; Jung, K.-H. *Chem. Phys. Lett.* **1997**, *265*, 573.
(17) Zoval, J.; Imre, D.; Ashjian, P.; Apkarian, V. A. *Chem. Phys. Lett.* **1992**, *197*, 549.
(18) Zoval, J.; Apkarian, V. A. *J. Phys. Chem.* **1994**, *98*, 7945.
(19) Khriachtchev, L.; Pettersson, M.; Isoniemi, E.; Räsänen, M. *J. Chem. Phys.* **1998**, *108*, 5747.
(20) Lechuga-Fossat, L.; Flaud, J.-M.; Camy-Peyret, C.; Johns, J. W. C. *Can. J. Phys.* **1984**, *62*, 2, 1889.
(21) Barnes, A. J.; Howells, J. D. R. *J. Chem. Soc., Faraday 2* **1972**, *68*, 729.
(22) Pacansky, J.; Calder, V. *J. Chem. Phys.* **1970**, *53*, 4519.
(23) Tang, S.-Y.; Brown, C. W. *J. Raman Spectrosc.* **1974**, *2*, 209.
(24) Nelander, B. *J. Chem. Phys.* **1978**, *69*, 3870.
(25) Barnes, A. J.; Bentwood, R. M.; Wright, M. P. *J. Mol. Struct.* **1984**, *118*, 97.
(26) Isoniemi, E. M.Sc. Thesis, University of Helsinki, Apr 1998.
(27) Koga, K.; Takami, A.; Koda, S. *Chem. Phys. Lett.* **1998**, *293*, 180.
(28) Acquista, N.; Schoen, L. J. *J. Chem. Phys.* **1970**, *53*, 1290.
(29) Barnes, A. J.; Hallam, H. E.; Howells, J. D. R. *J. Mol. Struct.* **1974**, *23*, 463.
(30) Catalano, E.; Milligan, D. E. *J. Chem. Phys.* **1959**, *30*, 45.
(31) Glasel, J. A. *J. Chem. Phys.* **1960**, *33*, 252.
(32) Redington, R. L.; Milligan, D. E. *J. Chem. Phys.* **1962**, *37*, 2162.
(33) Redington, R. L.; Milligan, D. E. *J. Chem. Phys.* **1963**, *39*, 1276.
(34) Ayers, G. P.; Pullin, A. D. E. *Chem. Phys. Lett.* **1974**, *29*, 609.
(35) Engdahl, A.; Nelander, B. *J. Mol. Struct.* **1989**, *193*, 101.
(36) Forney, D.; Jacox, M. E.; Thompson, W. E. *J. Mol. Spectrosc.* **1993**, *157*, 479.
(37) Anderson, D. T.; Winn, J. S. *Chem. Phys.* **1994**, *189*, 171.
(38) Milligan, D. E.; Hexter, R. M.; Dressler, K. *J. Chem. Phys.* **1961**, *34*, 1009.
(39) Pimentel, G. C.; Bulanin, M. O.; Van Thiel, M. *J. Chem. Phys.* **1962**, *36*, 500.
(40) Cabana, A.; Savitsky, G. B.; Hornig, D. F. *J. Chem. Phys.* **1963**, *39*, 2942.
(41) Frayer, F. H.; Ewing, G. E. *J. Chem. Phys.* **1967**, *46*, 1994.
(42) Frayer, F. H.; Ewing, G. E. *J. Chem. Phys.* **1968**, *48*, 781.
(43) Allavena, M.; Rysnik, R.; White, D.; Calder, V.; Mann, D. E. *J. Chem. Phys.* **1969**, *50*, 3399.
(44) Teles, J. H.; Maier, G.; Hess, B. A. Jr.; Schaad, L. J.; Winnewisser, M.; Winnewisser, B. P. *Chem. Ber.* **1989**, *122*, 753.
(45) Apkarian, V. A.; Weitz E. *J. Chem Phys.* **1982**, *76*, 5796.
(46) Schallmoser, G.; Thoma, A.; Wurfel, B. E.; Bondybey, V. E. *Chem. Phys. Lett.* **1994**, *219*, 101.
(47) Hallam, H. E. *Vibrational Spectroscopy of Trapped Species*, 1st ed.; John Wiley & Sons: London, 1973.
(48) Devonshire, A. F. *Proc. R. Soc. London Ser. A* **1936**, *153*, 601.
(49) Flygare, W. H. *J. Chem. Phys.* **1963**, *39*, 2263.
(50) Sauer, P. *Z. Phys.* **1966**, *194*, 360.
(51) King, H. F.; Hornig, D. F. *J. Chem. Phys.* **1966**, *44*, 4520.
(52) Miller, R. E.; Decius, J. C. *J. Chem. Phys.* **1973**, *59*, 4871.
(53) Muller, E.; Hyne, J. B. *Can. J. Chem.* **1968**, *46*, 2341.
(54) Our ab initio calculations for H_2S, $(H_2S)_2$, and $H_2S\cdots H_2O$ at the MP2/6-311++G(2d,2p) level indicate absorption intensities over 2 orders of magnitude greater on the symmetric stretch (ν_1) of the electron acceptor of $(H_2S)_2$ and in the $H_2O\cdots HSH$ complex than for the H_2S monomer. The absorption intensities for the $H_2S\cdots HOH$ complex are similar to those for the H_2S monomer.
(55) Yamada, K. M. T.; Klee, S. *J. Mol. Spectrosc.* **1994**, *166*, 395.
(56) Hollas, J. M. *High-Resolution Spectroscopy*, 1st ed.; Butterworth: London, 1982; Chapter 4.
(57) Khriachtchev, L.; Pettersson, M.; Räsänen, M. *Chem. Phys. Lett.* **1998**, *288*, 727.
(58) Pathak, C. M.; Palmer, H. B. *J. Mol. Spectrosc.* **1969**, *32*, 157.
(59) Pettersson, M.; Lundell, J.; Khriachtchev, L.; Isoniemi, E.; Räsänen, M. *J. Am. Chem. Soc.* **1998**, *120*, 7979.
(60) Allen, H. C., Jr.; Plyler, E. K. *J. Chem. Phys.* **1956**, *25*, 113.